Supercontinuum Broadband Laser Absorption Spectroscopy for Spatially Resolved Methane Measurements in Combustion Environments

N. G. Blume[1], V. Ebert[2,3], A. Dreizler[2], S. Wagner[*,1]

[1]High Temperature Process Diagnostics, Technische Universität Darmstadt, Germany
[2]Department of Reactive Flows and Diagnostics, Technische Universität Darmstadt, Germany
[3]Physikalisch-Technische Bundesanstalt, Braunschweig, Germany

Abstract
In this work the application of Supercontinuum Broadband Laser Absorption Spectroscopy (SCLAS) for quantitative measurement of methane mole fractions in an atmospheric, laminar, non-premixed CH_4/air flame (Wolfhard-Parker burner) is presented. Along with measurements and data evaluation a novel broadband fitting algorithm is described which allows the automatic recognition and fitting of a B-spline baseline of SCLAS broadband measurements. The comparison of the measured absolute mole fraction profile with experimental validation data showed excellent agreement in position, shape and absolute values of the methane profile.

Introduction

During recent years, several stricter legislative regulations of pollutant emissions as well as the constant need for energy efficiency improvements have led to increased efforts in understanding and improving combustion processes and designs. Along with these efforts, the need for extensive knowledge of the conditions while combustion takes place has yielded an increased demand for advanced in-situ species concentration measurements. Several techniques have been proven feasible and useful in the combustion context, among others the *Tunable Diode Laser Absorption Spectroscopy* (TDLAS) [1], as well as *coherent anti-Stoke Raman spectroscopy* (CARS) [2], *Raman-Rayleigh scattering* or *laser induced fluorescence* (LIF) [see 3 for general review]. For the application of such techniques to harsh industrial environments it is essential that these diagnostics operate with minimal optical access and are highly robust. Furthermore for the use of these techniques for process control purposes, the systems need to provide real-time data evaluation as well as high reliability and preferably very little or no sensor calibration at all. As previously shown [4,5,6], TDLAS fulfills the above mentioned demands and was already successfully applied even to very harsh combustion environments.

Since TDLAS, however, usually utilizes only a small number of absorption lines, excessive line broadening in high pressure processes can cause problems. Therefore the TDLAS approach has been expanded by the implementation of *vertical-cavity surface-emitting laser* (VCSEL) diodes, which provide continuous tuning ranges of up to 15 cm^{-1}, which is significantly larger than the very frequently used DFB lasers with up to 3cm^{-1} tuning range. TDLAS based on VCSEL laser diodes has already been applied to combustion processes [7]. Future enhancements of absorption based approaches therefore require the development of novel measurement techniques to allow for the recording of broadband spectra with high spectral resolution. This would allow for the simultaneous determination of multiple species concentrations as well as additional combustion parameters (i.e. temperature or pressure).

Recently, a very promising technique for recording broadband absorption spectra called *Supercontinuum Laser Broadband Absorption Spectroscopy* (SCLAS) has been demonstrated [8]. For this approach a spectrally broad, pulsed light source is used in connection with a strongly dispersing fiber. The ns to fs short but spectrally broad pulses (400 to 2400 nm) are dispersed in time prior to their modulation by absorption. The resulting light pulse is recorded with a high-speed high-bandwidth photodiode. The intensity information in the time-domain is transferred to the frequency-domain by correlating instants in time with the according wavelengths. To gain this correlation precise knowledge of the fiber dispersion is necessary and the quality of this correlation has an important influence on the system performance. The development of this technique was driven by recent improvements in the generation of supercontinuum laser light using PCFs (Photonic Crystal Fibers). Originally described by Orofino and Unterleitner in 1976 [9], this technique required several improvements in the field of photodiodes and electronic signal processing as well as the generation of pulsed broadband laser light sources prior to its successful implementation. Since it is based on light sources with high repetition rates of up to several 10 MHz it is a promising and versatile high-speed combustion diagnostic. So far, SCLAS has been applied to different environments, such as gas absorption cells [10] or flat-flame laminar burners [11].

In this work, we present the application of the SCLAS approach to a Wolfhard-Parker burner (WHP, atmospheric, laminar, non-premixed CH_4/air flame

[*] Corresponding author: wagner@csi.tu-darmstadt.de
Proceedings of the European Combustion Meeting 2015

consisting of two flame sheets) [12]. This burner requires a single-pass setup allowing only an absorption path length of 41 mm as opposed to multi-pass setups used previously.

The measured spectra are evaluated quantitatively with a novel broadband fitting algorithm. Absolute mole fraction profiles are compared to reference measurements by Norton et al. [13] for quantitative validation.

Optical Setup

The measurement setup consisted of a *supercontinuum laser light source* (SCL) with a spectral coverage ranging from 400 to 2400 nm and repetition rates from 2 MHz to 80 MHz (NKT SuperK EXTREME). The output of the SCL was split at 1000 nm to remove the visible spectrum and furthermore filtered by a dichroic mirror specifically designed to transmit NIR wavelengths from 1200 to roughly 1800 nm. The remaining light was coupled into a single-mode fiber and dispersed by a *Dispersion Compensating Module* with a dispersion of -1.493 ns/nm at 1550 nm. The dispersion was characterized using a time-of-flight based approach and found to closely match the value of 1.50 ns/nm measured by the manufacturer (see Figure 1).

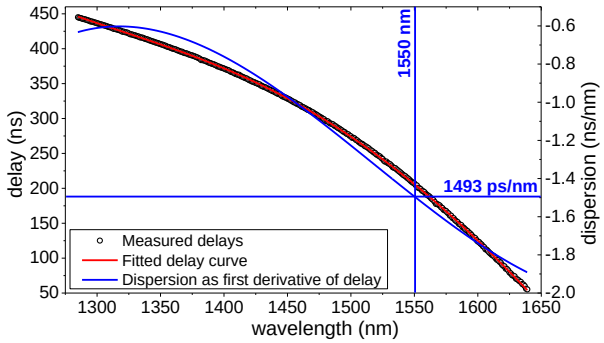

Figure 1 Dispersion curve of the DCM used in the experiment determined by a time-of-flight measurement technique [Circles: Measured delays; Red: Fitted delay curve; Blue: Dispersion as first derivative of the delay measured].

Following the dispersion fiber, the light was collimated and sent through the absorption region, where the spectrum is modulated by the absorbing species along the absorption path (for details see experimental setup). After the absorption region, the light was coupled back into a multi-mode fiber via a periscope and then detected by an amplified high-speed InGaAs photodiode (12 GHz bandwidth). This signal was sampled by a high speed oscilloscope (LeCroy 20 GHz bandwidth). Using the processing capabilities of the oscilloscope, a number of pulses was recorded and averaged (for this study 9850 pulses with a repetition rate of 2 MHz were averaged, resulting in a spectrum repetition rate of 203 Hz). The complete SCLAS setup is shown in Figure 2. Based on a procedure discussed by Sanders [14], the spectral resolution of the system was calculated to be 0.159 cm^{-1} around 1675 nm.

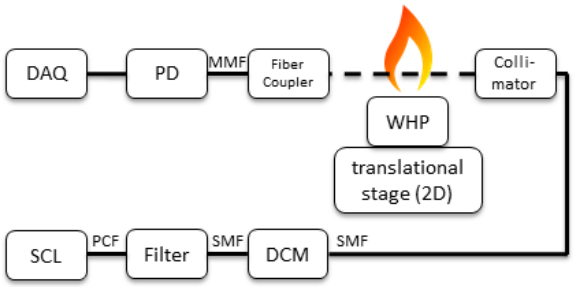

Figure 2 System setup of the SCLAS measurement system applied to a WHP burner mounted on a 2D translational motion stage

To specify the spectral content of the light pulses used in the experiments an emission spectrum was recorded (with and without the DCM) using a FTIR (Bruker VERTEX 80v) spectrometer with a TE cooled extended InGaAs detector (see Figure 3). For comparison a SCLAS trace of the same setup (including the DCM) is shown as well, on a separate axis (time). For all three cases the intensity was individually normalized. Clearly visible are the oscillations in filter transmittance due to the dichroic coating of the filters used to select the proper part of the spectrum. These oscillations in combination with ringing of the photodiode, which is characteristic for pulse measurements, can be seen in the recorded traces later on and will be addressed in the broadband fitting algorithm. Due to the transmission characteristic of the DCM module, wavelengths towards 1700 nm are attenuated and blocked above 1700 nm. Due to the different responsivities of the two InGaAs detectors, the intensity trace of the SCLAS measurement varies compared to the FTIR measurement.

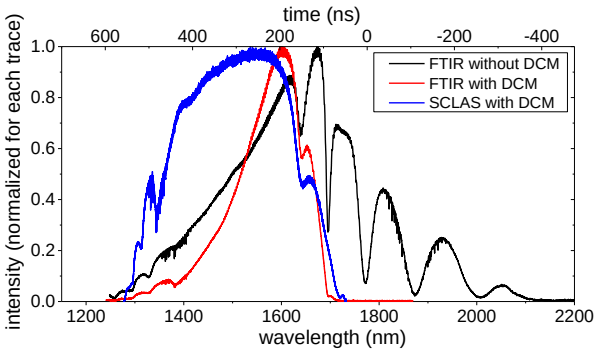

Figure 3 Spectral content of SCL pulses after filtering and transmittance through the DCM (where indicated) [Red, Black: Bruker VERTEX 80v with ext. TE-InGaAs detector; Blue: SCLAS setup with DCM and high-speed InGaAs detector].

Experimental Setup and Details

For the experiments a modified Wolfhard-Parker burner design, as described in detail in [15], was used. The modified WHP burner consisted of a central slot ejecting methane and providing a quasi-homogeneous single-path absorption length of only 41 mm. Parallel to the central methane slot, air was provided by two

adjacent slots. To suppress end-flames the burner was equipped with nitrogen purge slots at each end of the methane slot as shown in Figure 4. The two diffusion flame sheets were stabilized against a wire screen chimney. Flame stability was further enhanced by shielding the flame against any ventilation in the lab. The complete setup was mounted on a 2-axis motion stage to allow for precise positioning of the flame to the laser beam.

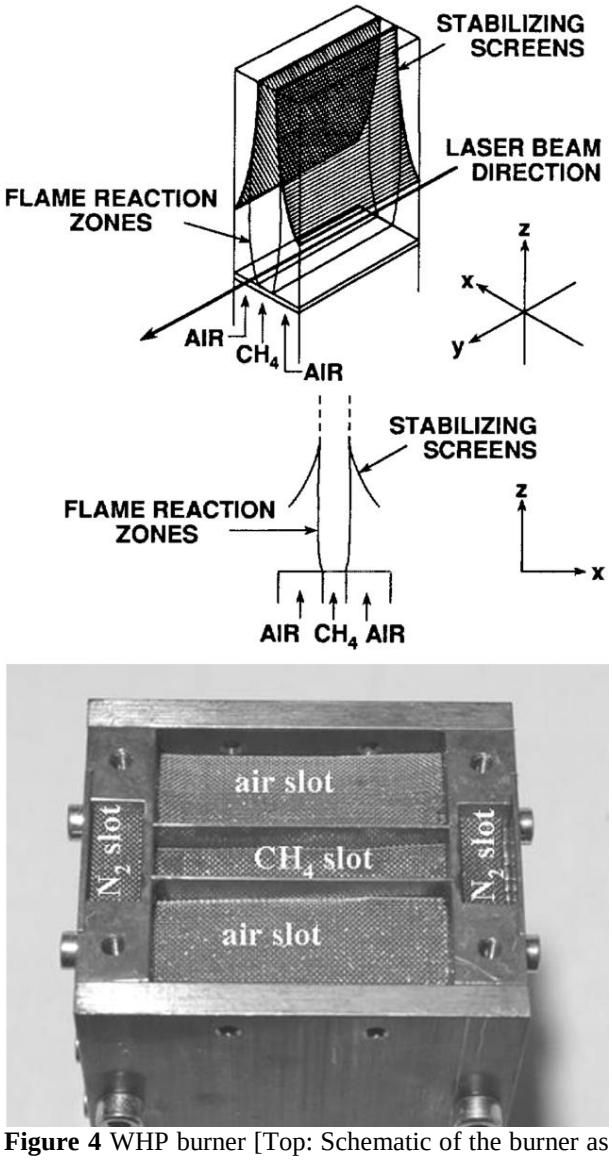

Figure 4 WHP burner [Top: Schematic of the burner as previously used by [12,15]; Bottom: Photograph of the modified version of the WHP burner equipped with additional N_2 purge slots. During the operation the top portion of the burner was covered with a second layer of copper screen.].

The WHP burner was operated comparable to previous reference measurements [12,13,15], i.e. with a CH_4 exit velocity of 11 cm/s and air and N_2 velocities of 22 cm/s. Using the translation stage, measurements were taken at different lateral positions along the x-axis (see Figure 4 for reference frame). All measurements were taken at a height of 7 mm above the burner surface and with a collimated beam diameter of 0.4 mm.

To properly correlate the measurements with the reference provided by Norton et al. [13], measurements were conducted for two different conditions (each with steps of 0.1 mm lateral spacing). In the first case, additionally to the air and nitrogen flows, the methane flow was activated, but not ignited (*cold methane* in mixture with air and nitrogen). For the second case, the burner was operated in its nominal state with an actively burning flame (*hot methane*).

Broadband Fitting Algorithm

In previous work TDLAS has been utilized for measurements in complex environmental and process conditions. To allow for determination of species concentration and other parameters under these conditions advanced data post-processing algorithms were developed and validated against national standards [16,17]. Due to the spectral width inherent to TDLAS systems these algorithms were optimized for fitting small sets of spectral lines documented in databases such as HITRAN. In the context of SCLAS, and in contrast to TDLAS, the spectral width can easily exceed hundreds of wavenumbers which results in the need to include hundreds, if not thousands of spectral lines in the fitting process (each modeled with a Voigt form function). In TDLAS, the baseline intensity can be modeled with a lower order polynomial depending on the laser and modulation used. Furthermore the correlation between instants in time along the TDLAS scan ramp and the according wavelengths emitted by the laser diode, can be determined by an etalon [18]. This correlation typically is very stable and can be understood as characteristic for the laser diode and tuning, since it often can be used several years later without re-characterization. In SCLAS systems, however, these features need to be handled differently due to the very different nature of such a system. To address these differences the novel broadband fitting algorithm was developed, which in part is based on the previous experience with TDLAS systems, but incorporates several new features and techniques to address SCLAS-specific needs and problems. This algorithm is currently under further development and will be expanded in the future to fully utilize the capabilities of a SCLAS system (i.e. multi-species multi-parameter datasets).

In Figure 5 an exemplary measurement trace of cold methane is shown. In addition to the methane spectrum, water lines are clearly visible in the time interval between 400 and 500 ns. This trace is used in the following to discuss the different features of the fitting algorithm. It is obvious that a baseline fit covering the entire spectrum is not easily possible. Furthermore, in sections where multiple lines interfere with each other determination of the background is further complicated.

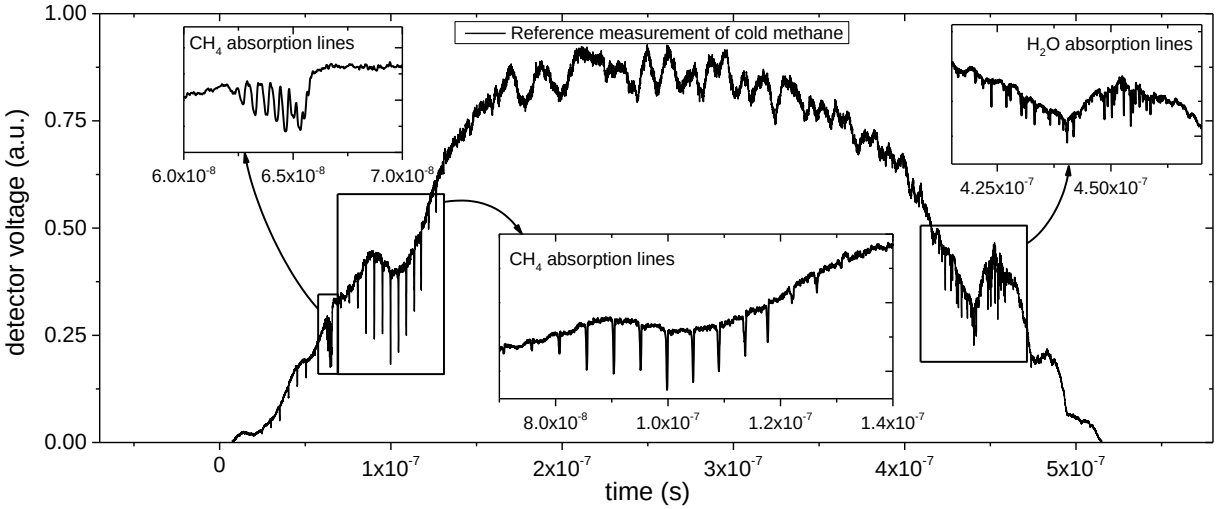

Figure 5 Exemplary measurement trace of cold methane showing the need for a non p-order polynomial baseline as well as highly resolved spectral lines and additional water lines present on the signal. Due to the negative dispersion of the DCM longer wavelength arrive at the photodiode before shorter wavelength.

Since the baseline intensity of SCLAS traces cannot necessarily be represented with p-order polynomials, for this algorithm a B-Spline is fitted (see Figure 6). Using a simple least square error fit, the peaks of the absorption lines would be treated as deviations from the baseline to be fitted. This would be interpreted as an apparent error with significant influence upon the baseline fit. To avoid this bias by the absorption lines, prior to the B-spline fit of the baseline, the absorption peaks are removed. For this purpose those spectral sections are identified by fitting Lorentzian functions to the absorption peaks and using a multiple of the FWHM peak width as the width of the removed section.

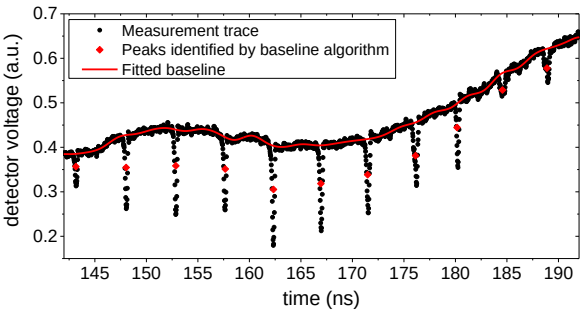

Figure 6 Exemplary baseline trace determined by the novel broadband fitting algorithm described in this work.

As with TDLAS systems, a correlation of time and wavenumber needs to be determined to convert the recorded signal from the time domain to the frequency domain. For SCLAS data processing this correlation needs to be known precisely, since a slight error or non-sufficient precision of a coefficient can result in strong line position errors during the fitting process. It is difficult to correct these errors afterwards during the fitting process. To address this issue, our new broadband fitting algorithm employs three process steps. Firstly, using the measured dispersion curve, a rough estimate of the time-wavenumber correlation is generated. Secondly, the absorption lines in the measured trace are located and coarsely fitted with Lorentzian profile functions to determine the peak line positions in the time domain. Based on a simulated reference spectrum of the analyte species, the corresponding peak positions are identified and also fitted with Lorentzian peaks but in the spectral domain. Finally, the corresponding line positions in time and wavenumber space are correlated using a polynomial of order *p*. To further improve this correlation this last fit is iterated twice. Based on this time-wavenumber correlation the data is converted from temporal to the spectral domain (termed herein “transferred trace”). The transferred trace (wavenumber vs. absorbance) is then fitted against a line-set from HITRAN 2012 [19] with spectral position, area and collision width adjusted freely by the fit.

Absolute methane mole fractions were extracted from the resulting line areas by using the evaluation procedure developed for calibration-free direct absorption spectroscopy [18].

Results and Discussion

Using the setup described above two sets of measurements were recorded: Measurements of unignited *cold methane* were used to spatially correlate the lateral positions with the reference frame used by Norton et al. [13]. Based on this spatial correlation the hot methane (flame) measurements were evaluated and compared to the according measurements as well.

An exemplary measurement (lateral position x = 0.0 mm) of absolute CH_4 mole fraction is shown for the *cold methane* case in Figure 7. The peaks in the residuum of the fitted spectrum are caused primarily by photo diode ringing, especially on the shorter wavelength side of an absorption peak (as mentioned earlier). This phenomenon is characteristic for high-bandwidth high-speed photo diodes, since their response to short pulses includes a certain overshoot and

oscillation. For the final fit we used a total number of 695 CH_4 absorption lines ranging from 6030 cm^{-1} to 6140 cm^{-1}. The standard deviation of the complete residual is $2.2x10^{-2}$, while the standard deviation omitting the areas influenced by absorption peaks is $7.6x10^{-3}$. Using the later value of the standard deviation this yields a peak SNR of 140 for *cold methane* using the strongest absorption line. Based on the peak SNR a mole fraction error of approximately 0.6 Vol.-% is estimated, resulting in a normalized sensitivity of 17.3 ppm·m·$(Hz)^{-0.5}$ at 300 K.

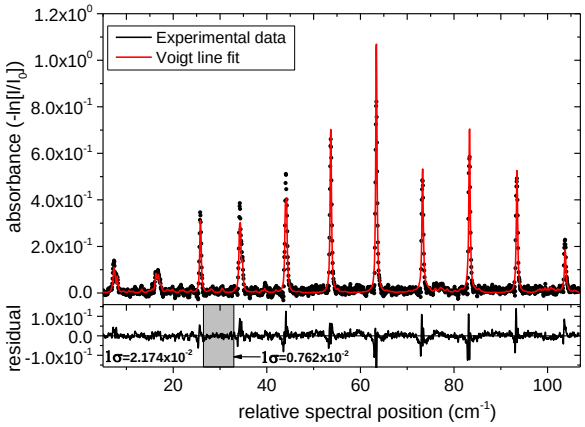

Figure 7 Measurement and fitted spectrum for *cold methane* at lateral position x = 0.0 mm (at p=1000 mbar, T=297 K) using the HITRAN 2012 database. With an SNR of 140 we determined an absolute CH_4 mole fraction to 83.96 Vol.-% (+/- 0.6 Vol-%).

For the combusting case providing *hot methane* in the vicinity of the heat release zones an exemplary measurement at the lateral position x = 0.0 mm is shown in Figure 8. Based on reference measurements [12] the temperature for this location was determined as 473 K. The temperatures for all other measured lateral positions were determined accordingly ranging from 473 K up to 1230 K. As with *cold methane*, 695 CH_4 absorption lines were used covering the same spectral region as before. Based on the fitted spectral region the standard deviation is $1.3x10^{-2}$, while the local standard deviation is $9.2x10^{-3}$. Based on the strongest absorption line this yielded a SNR of 46, resulting in a mole fraction error of 1.9 Vol-%. Compared to the measurements of *cold methane* the global standard deviation is in the same order of magnitude. Due to the smaller peak absorption the effect of photo diode ringing is diminished in the case of *hot methane*. Since the local temperature is essential for the proper calculation of the according mole fraction, future extensions of the broadband fitting algorithm will focus on deriving the temperature based on water absorption lines in the signal itself.

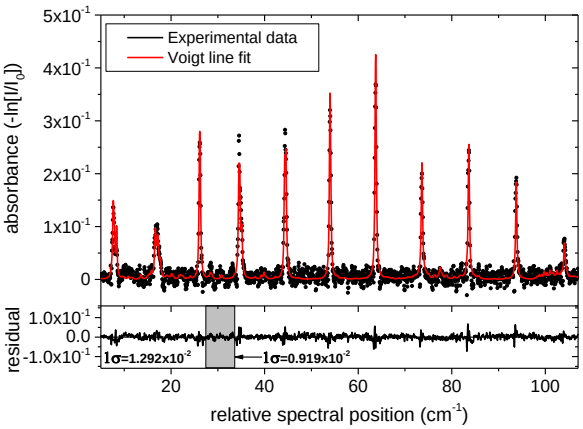

Figure 8 Measurement and fitted spectrum for *hot methane* at lateral position x = 0.0 mm (at p=1000 mbar, T=473 K) using the HITRAN 2012 database. With an SNR of 46 we could determine the absolute mole fraction to 86.6 Vol-% (+/- 1.9 Vol-%).

To compare shape and spatial distribution of the CH_4 mole fraction we determined CH_4 mole fractions at different positions along the lateral axis in steps of 0.1 mm as previously described in detail for a single position. Figure 9 shows the derived CH_4 spatial profile for *cold methane*. Based on this measurement the lateral positions were correlated to the frame of reference for the measurements taken from [12]. The variation of the methane concentration is consistent with the non-ignited mode of operation of the WHP burner (showing mixing effects and symmetrical distribution).

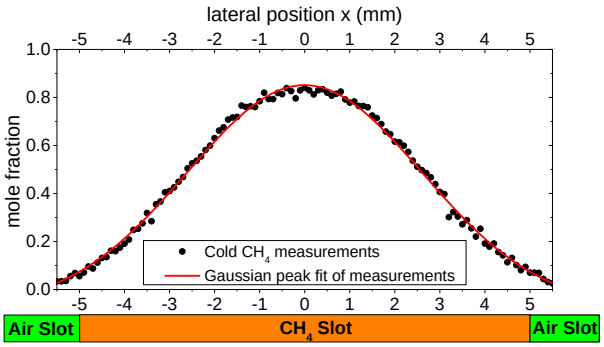

Figure 9 Spatially resolved measurements of unburned methane (CH_4) of the WHP burner

For the combusting case with *hot methane* located in the central region of the flow absolute CH_4 mole fraction measurements are shown in Figure 10. The resulting shape, position and absolute values for CH_4 mole fraction closely match the values obtained by Norton et al. [12] for methane concentrations in the flame of the WHP burner. Towards the outer wings of the concentration distribution a slight underestimation of the mole fraction is obvious. Possible reasons beside minor differences in the flow field include distortion of the absorption line function (given the photodiode ringing described earlier) and issues with the baseline determination.

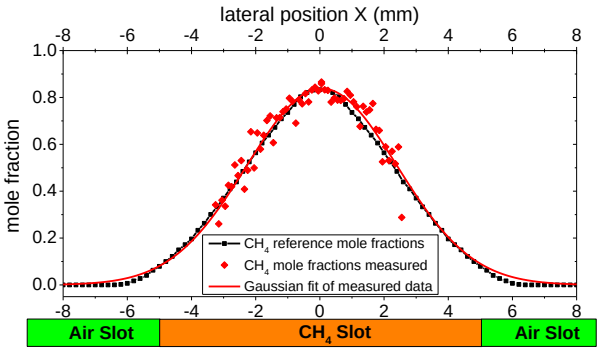

Figure 10 Spatially resolved measurements of unburned methane (CH_4) of the WHP burner

In general the overall results closely match the reference values and therefore validates that our SCLAS based sensing approach can be utilized for spatially resolved quantitative measurements in combustion environments with single-path setups and short absorption path lengths (41 mm in this case).

Conclusions and Outlook

Using the novel diagnostic SCLAS system, spatially resolved broadband quantitative species concentration measurements were performed on a WHP burner for methane (CH_4) with a single-path setup and an absorption length of 41 mm. These measurements were found to closely match previous experimental reference values for this burner setup. Our broadband multiline fitting algorithm has been proven to greatly enhance the performance of the overall fit and the quality of the results as well.

During this work, several areas of improvement for SCLAS were identified, including photo diode ringing and SCL-generation inherent noise. In future the system will be applied to high pressure environments (absorption cell with elevated pressures) and fast pressure transients to utilize the advantages of the broader spectral coverage of SCLAS in the context of high pressure environments.

Acknowledgements

This work was supported in part by the UNICO program at TU Darmstadt and the Deutsche Forschungsgemeinschaft through SFB/Transregio 129 project B05.

References

[1] C. Schulz, A. Dreizler, V. Ebert, J. Wolfrum, in: C. Tropea, A. L. Yarin, & J. F. Foss (Eds.), Handbook of Experimental Fluid Mechanics, Springer, Berlin Heidelberg, 2007, p. 1241-1316.
[2] S. Roy, J.R. Gord, A.K. Patnaik, Prog. Energy Combust. Sci. 36 (2010) 280–306
[3] K. Kohse-Höinghaus, R.S. Barlow, M. Aldén, J. Wolfrum, Proc. Combust. Inst. 30 (2005) 89–123
[4] H. Teichert, T. Fernholz, V. Ebert, Applied Optics 42 (2003) 2043–2051
[5] V. Ebert, H. Teichert, P. Strauch, T. Kolb, H. Seifert, J. Wolfrum, Proc. Combust. Inst. 30 (2005) 1611-1618
[6] S. Wagner, M. Klein, T. Kathrotia, U. Riedel, T. Kissel, A. Dreizler, V. Ebert, Appl. Phys. B 107 (2012) 585–589
[7] O. Witzel, A. Klein, C. Meffert, S. Wagner, S. Kaiser, C. Schulz, V. Ebert, Optics Express 17 (2013) 19951-19965
[8] C.F. Kaminski, R.S. Watt, A.D. Elder, J.H. Frank, J. Hult, Appl. Phys. B 92 (2008) 367-378
[9] T. Orofino, F. Unterleitner, Appl. Opt. 15 (1976) 1907-1909
[10] R.S. Watt, C.F. Kaminski, J. Hult, Appl. Phys. B 90 (2007) 47-53
[11] T. Werblinski, F. Mittmann, M. Altenhoff, T. Seeger, L. Zigan, S. Will, Appl. Phys. B 118 (2014) 153-158
[12] J.H. Kent, H. Jander, H.Gg. Wagner, Comb. Symp. 18 (1981) 1117-1126
[13] T.S. Norton, K.C. Smyth, J.H. Miller, M.D. Smooke, Combust. Sci. Technol. 90 (1993) 1-34
[14] S. T. Sanders, Appl. Phys. B Lasers Opt. 75 (2002) 799-802
[15] S. Wagner, B. T. Fisher, J. W. Fleming, V. Ebert, Proc. Combust. Inst. 32 (2009) 839-846
[16] E. Schlosser, J. Wolfrum, L. Hildebrandt, H. Seifert, B. Oser, V. Ebert, Appl. Phys. B Lasers Opt. 75 (2002) 237–247
[17] B. Buchholz, N. Böse, V. Ebert, Appl. Phys. B 116 (2014) 883-899
[18] E. Schlosser, T. Fernholz, H. Teichert, V. Ebert, Spectrochim. Acta. A. 58 (2002) 2347-2359
[19] L.S. Rothman, I.E. Gordon, Y. Babikov, A. Barbec, D. Chris Benner, P.F. Bernath, M. Birk, L. Bizzocchi, V. Boudon, L.R. Brown, A. Campargue, K. Chance, E.A. Coheni, L.H. Coudert, V.M. Devi, B.J. Drouin, A. Fayt, J.-M. Flaud, R.R. Gamache, J.J. Harrison, J.-M. Hartmann, C. Hill, J.T. Hodges, D. Jacquemart, A. Jolly, J. Lamouroux, R.J. Le Royr, G. Li, D.A. Long, O.M. Lyulin, C.J. Mackie, S.T. Massie, S. Mikhailenko, H.S.P. Müller, O.V. Naumenko, A.V. Nikitin, J. Orphal, V. Perevalov, A. Perrin, E.R. Polovtseva, C. Richard, M.A.H. Smith, E. Starikova, K. Sung, S. Tashkun, J. Tennyson, G.C. Toon, Vl.G. Tyuterevc, G. Wagner, J. Quant. Spectrosc. Radiat. Transfer, 130 (2013) 4-50